http://dx.doi.org/10.1016/j.jtbi.2014.09.014

Estimating and determining the effect of a therapy on tumor dymamics by means of a modified Gompertz diffusion process

Giuseppina Albano[a], Virginia Giorno[b], Patricia Román-Román[c], Sergio Román-Román[d], Francisco Torres-Ruiz[c]

[a] Dip. di Scienze Economiche e Statistiche, Università di Salerno, Italy

[b] Dip. di Studi e Ricerche Aziendali (Management and Information Technology), Università di Salerno, Italy

[c]Dpto. de Estadística e Investigación Operativa, Universidad de Granada, Spain

[d]Dép. de Recherche Translationnelle, Institut Curie, France

Abstract

A modified Gompertz diffusion process is considered to model tumor dynamics. The infinitesimal mean of this process includes non-homogeneous terms describing the effect of therapy treatments able to modify the natural growth rate of the process. Specifically, therapies with an effect on cell growth and/or cell death are assumed to modify the birth and death parameters of the process. This paper proposes a methodology to estimate the time-dependent functions representing the effect of a therapy when one of the functions is known or can be previously estimated. This is the case of therapies that are jointly applied, when experimental data are available from either an untreated control group or from groups treated with single and combined therapies. Moreover, this procedure allows us to establish the nature (or, at least, the prevalent effect) of a single therapy in vivo. To accomplish this, we suggest a criterion based on the Kullback-Leibler divergence (or relative entropy). Some simulation studies are performed and an application to real data is presented.

Keywords: Tumor dynamics, Gompertz diffusion process, Therapy effect estimation, Kullback-Leibler divergence, Resistor average distance

1 Introduction

In the last decades, increasing attention has been paid to the formulation and analysis of mathematical procedures for modeling tumor growth and the effect of therapies in cancer animal models. Innovative and informative analytical methods modeling tumor growth in vivo could result in more accurate interpretation of data obtained from these animal models, and help pharmacologists to adapt administration schedules of drugs at the preclinical setting. Moreover such tools could also potentially give insights into the mechanism of action of the drugs in vivo. Actually, mechanistic studies of drugs are conducted in vitro and both the host and the tumor microenvironment can dramatically affect the mechanism by which a given drug or drug combination is displaying its activity in vivo.

In a first approach, the models are related to a particular growth curve that is a solution of a differential equation. The deterministic models more commonly used in the study of tumor growth are the Malthusian (associated with the exponential curve) and those related to sigmoidal curves as the logistic or Gompertz. This second model is the most widely accepted to capture

dynamics in solid tumors (see the classic work of Norton [25], or that of Gerlee [15] for a recent historical perspective). In order to take into consideration the environmental fluctuations that are often cause of discrepancies between preclinical data and theoretical predictions, the notion of growth in random environment has been formulated (see, for instance, [26] and references therein).

Various approaches (deterministics and stochastics), based on the population dynamics, are proposed in literature to analyze tumor growth. Essentially, these approaches consist in the formulation and analysis of models of various natures that can be summarized as follows:

- deterministic models describing the dynamics of a single population. In this context the study is oriented to the estimation of the involved growth parameters (cf. [27]) to analyze the effect of specific therapies (cf. [19]);
- deterministic prey-predator type models describing the interaction of immune system cells (predator) and cancer cells (prey) (cf. [3], [12], [13], [32]);
- stochastic models for cancer dynamics that take into account both cell fission and mortality (cf. [20], [21]);
- stochastic models describing the effects of therapies that slow the growth according of continuous functions of the time (cf. [2], [4], [6], [30]) or influence it by inducing some instantaneous jumps (cf. [18]),
- stochastic models allowing the estimation of parameters involved in the tumor dynamics (cf. [4], [5]).

Experimental design to test the effectiveness of therapeutic treatments includes untreated (control) and treated groups in which the progress of the tumor size is evaluated through the time. This paper addresses experimental studies of tumor growth in mice following the approach of the diffusion processes by considering the tumor growth data observed in each mouse as a sample path of the process. We work under the assumption that the tumor growth in the control group adequately fits with a Gompertz diffusion process. This process is obtained by including random environment in the deterministic Gompertz model given by the differential equation

$$dx(t) = [\alpha x(t) - \beta x(t) \ln x(t)]dt, \qquad x(t_0) = x_0,$$

with α and β positive constant (representing the birth and death parameters respectively). Thus, the Gompertz diffusion process is defined by means of the stochastic differential equation

$$dX(t) = [\alpha X(t) - \beta X(t) \ln X(t)]dt + \sigma X(t)dW(t), \qquad X(t_0) = X_0, \tag{1.1}$$

where $\sigma > 0$ measures the width of the random fluctuations, $W(t)$ is a standard Brownian motion and X_0 is a positive random variable independent from $W(t)$ for all $t \geq t_0$.

The effect of a given therapy can be included in the model by assuming that the growth parameters are time-dependent functions. Thus, the study of tumor growth under the effect of a treatment can be approached by means of a modification of the process fitted to the control group.

The knowledge of these functions should allow to evaluate the effectiveness of a treatment throughout time, and also to better establish treatment schedules. However, in experimental studies is not obvious to deduce the effect of therapies on cancer dynamics, i.e. how they are capable of modifying the growth rate of tumor cells. By generalizing a previous model (see [2],

[4]), in which we analyzed the effect of an anti-proliferative therapy (that modifies the birth rate of the cancer population), now we consider a model in which the death rate of the tumor cells is also affected. The interest of the formulation of such a model relies on the existence of drugs displaying both antiproliferative effect (reducing the birth rate) and pro-apoptotic or senescence action (increasing the death rate) as, for example, some anti-angiogenic and anti-estrogen drugs (cf. [9], [10]).

Therefore, it would be very interesting to determine if tumor growth inhibition observed in vivo with drugs or drug combination is occurring by affecting cell death, cell proliferation or both. The comprehension of mechanisms by which drug combination act in vivo is crucial. Resistance to chemotherapy or targeted therapies in cancer patients is a major issue and recent preclinical and clinical studies have shown that many patients might benefit of drug combination approaches. Some examples are the combination of BRAF and EGFR inhibitors in BRAF-mutated colorectal cancer cells ([28]), combination of BRAF and MEK in BRAF mutated cutaneous melanoma patients ([14]) or association of everolimus with hormonotherapy in breast cancers ([7], [8]).

In the present paper we propose a methodology to estimate the dependent functions representing the effect of a therapy (which can affect growth and/or death rate) when one of the functions is known or can be estimated previously. This is the case when therapies are jointly applied and experimental data of either an untreated control group and groups treated with single and combined therapies, are available. Moreover, this procedure allows to establish the nature (or, at least, the prevalent effect) of a single therapy in vivo.

The paper is organized as follows. In Section 2 we introduce the model with some of its main characteristics. In Section 3 we provide a procedure, essentially based on the geometric mean of the process, to estimate the time dependent functions representing the effect of the therapies. Moreover, some criteria are considered in order to obtain insights into the nature of a therapy in experimental studies. Some simulation results are developed in Section 4 in order to show the validity of the proposed procedure. A comparison with a previous procedure suggested in [4] is also discussed when both of them can be applied. Finally, in Section 5, an application to real data is presented. We have applied our methodology to data obtained in a patient-derived uveal melanoma xenografted in mice and challenged with drugs displaying different mechanisms of action.

2 The model

In this paper we assume that tumor growth in the control group of an experimental study adequately fits a Gompertz diffusion process (1.1).

To include the effect of an antitumoral treatment, exogenous terms can be included in the infinitesimal mean to account for modifications in the natural growth rate α and β and to represent tumor regression rate due to the application of therapy. Specifically, since α and β represent the birth and death parameters respectively, the inclusion of an additive term $-C(t)x$ modifies birth rate α by including the effect on cell growth, whereas the inclusion of an additive term $-D(t)x\ln x$ modifies the death rate β by including the cell death effect.

Thus, the resulting model is the time non-homogeneous diffusion process described by the stochastic differential equation

$$dX(t) = [(\alpha - C(t))X(t) - (\beta - D(t))X(t)\ln X(t)]dt + \sigma X(t)dW(t), \qquad X(t_0) = X_0, \quad (2.1)$$

where $C(t)$ and $D(t)$ are continuous functions in $[t_0, T]$. The diffusion process $X(t)$ is defined in $(0, +\infty)$ and characterized by drift and infinitesimal variance (cf. [1]):

$$A_1(x,t) = (\alpha - C(t))\, x - (\beta - D(t))\, x \, \ln x, \qquad A_2(x) = \sigma^2 \, x^2,$$

respectively.

Based on the interpretation of parameters α and β of a Gompertz curve, the interpretation of functions $C(t)$ and $D(t)$ is as follows:

- Negative values of $C(t)$ correspond to an increase in the growth rate of the group treated with respect to the control group, whereas positive values of $C(t)$ correspond to a decrease in the growth rate of the group treated with respect to the control group. Moreover, a decrease in tumor size takes place in the time intervals for which $C(t) > \alpha$.
- Negative values of $D(t)$ correspond to a deceleration in the growth rate of the group treated with respect to the control group, whereas positive values of $D(t)$ correspond to an acceleration in the growth rate of the group treated with respect to the control group.

2.1 Some characteristics

In this section, some of the main characteristics of the diffusion process defined by (2.1) are presented. Concretely, from the unidimensional distributions of the process, the moments and the geometric mean are obtained. The latter will facilitate computing the estimates of functions $C(t)$ and $D(t)$, included in the model. Finally, the expression of the transition probability density of the process, the solution of the corresponding Fokker-Plank equation, is also presented.

Assuming that X_0 is a lognormal random variable $\Lambda_1(\mu_0, \sigma_0^2)$, one has (see Appendix A for details):

$$X(t) \sim \Lambda_1(M(t|\mu_0, t_0), V^2(t|\sigma_0^2, t_0)), \tag{2.2}$$

where the general expressions for M and V are given by[1]

$$M(t|u,\tau) = \frac{k(\tau)}{k(t)}\, u + \frac{1}{k(t)} \int_\tau^t \left[\alpha - C(\theta) - \frac{\sigma^2}{2}\right] k(\theta)\, d\theta, \tag{2.3}$$

$$V^2(t|u,\tau) = \frac{1}{k^2(t)} \left[u + \sigma^2 \int_\tau^t k^2(\theta)\, d\theta\right], \tag{2.4}$$

with $k(t) = \exp\left\{\beta(t - t_0) - \int_{t_0}^t D(\theta)\, d\theta\right\}$.

From (2.2), one has the n-order moment of $X(t)$

$$\mathbb{E}[X^n(t)] = \exp\left\{n\, M(t|\mu_0, t_0) + \frac{n^2}{2}\, V^2(t|\sigma_0^2, t_0)\right\}.$$

In particular, the mean and the variance of $X(t)$ are given by

$$m_X(t) = \mathbb{E}[X(t)] = \exp\left\{M(t|\mu_0, t_0) + \frac{1}{2}\, V^2(t|\sigma_0^2, t_0)\right\} \tag{2.5}$$

[1] M and V are time functions used in the notation of the distributions of the process. In this sense, u and τ are fixed parameters of such distributions: τ indicates the fixed time instant for the transition distribution $X(t)|X(\tau)$ given by (2.7) (t_0 for the marginal distribution of $X(t)$ given by (2.2)); u indicates the parameters of the lognormal initial distribution for the marginal distribution, or the parameters of the lognormal distribution corresponding to a degenerate distribution in the value of the process at $X(\tau)$ for the transition distribution.

and

$$\sigma_X^2(t) = Var[X(t)] = m_X^2(t)\ \left[\exp\left\{V^2(t|\sigma_0^2, t_0)\right\} - 1\right],$$

and the geometric mean of $X(t)$ by

$$\mathcal{G}_X(t) = \exp\left\{M(t|\mu_0, t_0)\right\}. \tag{2.6}$$

Moreover, $X(t)|X(\tau) = y \sim \Lambda_1(M(t|\ln y, \tau), V^2(t|0, \tau))$, i.e. the transition probability density function of the process is:

$$f(x, t|y, \tau) = \frac{1}{x\sqrt{2\,\pi\,V^2(t|0,\tau)}}\ \exp\left\{-\frac{[\ln x - M(t|\ln y, \tau)]^2}{2\,V^2(t|0,\tau)}\right\}. \tag{2.7}$$

3 Determining and fitting the effect of therapies

Experimental studies to test the effectiveness of a therapeutic treatment usually include a control group and one (or more) treated groups, and tumor size is observed in both at established times. We assume that the control group is modeled by means of (1.1) and that the treated groups are described by (2.1), in which functions $C(t)$ and $D(t)$ are unknown and must be estimated.

This Section focuses on solving two important problems:

Problem 1 For each therapy applied, to determine its effect (which can affect growth and/or death rate) or, at least, to deduce its prevalent effect.

In this case, from data of the control (untreated) group and the group receiving therapy, in interval $[t_0, T]$, two models (with $C(t) = 0$ or $D(t) = 0$, $\forall t \in [t_0, T]$) will be estimated. Using appropriate criteria, the best one will be chosen.

Problem 2 Fitting the effects of two jointly-applied therapies (whose effects, one of them mainly affecting cell growth and the other mainly inducing cell death, are known or can be previously estimated).

The combined application of therapies can be carried out

a) from the initial time t_0 of experimentation or

b) by adding a therapy to the previous one from a subsequent time instant $t_0 < T^* < T$.

In the case b), data from the control (untreated) group (in $[t_0, T]$), from the group treated with the combined therapies (in $[T^*, T]$), and from the group treated with the first therapy applied (in $[t_0, T]$), are necessary. For the case a), which can be reduced to the second one (by considering or taking $T^* = t_0$), data are required from the untreated group and from the groups treated with single and combined therapies in $[t_0, T]$. In the following we will only consider the case b).

The solution of this problem requires two steps: firstly we estimate the term due to the first therapy applied (in the case b) or simply one of them (in the case a). Secondly, we estimate the term due to the second therapy applied (in the case b) or the other (in the case a) assuming that the first (other) term (C or D) is known.

Thus, in either problem it is enough to estimate one of the functions (C or D) when the other one is known. In addition, for the solution of problem 1 we need to establish a criterion for the selection of the effect type. We will address both problems below.

3.1 Estimation of functions $C(t)$ and $D(t)$

For the processes modeling the control group and the treated groups, let us suppose we have p sample paths, observed at the same time instants, $t_1, t_2, \ldots, t_n$, of the interval $[t_0, T]$. Let $\{x_{ij},\ i = 1, 2, \ldots, n;\ j = 1, 2, \ldots, p\}$ be the observed values of the sample paths.

Note that, from (2.6) we have, for the general model (2.1),

$$M(t|\mu_0, t_0) = \log \mathcal{G}_X(t).$$

Moreover, from (2.3) we can observe that the function $M(t|\mu_0, t_0)$ satisfies the differential equation:

$$\frac{d\, M(t|\mu_0, t_0)}{dt} = -(\beta - D(t))M(t|\mu_0, t_0) + \alpha - C(t) - \frac{\sigma^2}{2}. \tag{3.1}$$

Eq. (3.1) allows to implement the following procedure:

- From the data of the control group, estimate α, β and σ^2, obtaining $\widehat{\alpha}$, $\widehat{\beta}$ and $\widehat{\sigma^2}$.
- From the data of the group treated with the first therapy applied, in the time interval $[t_0, T]$ obtain the sample geometric mean of the process. Let g_j^1 be the geometric mean at $t_j \in [t_0, T^*]$.
- From the data of the group treated with the combined therapies in $[T^*, T]$, obtain the sample geometric mean of the process. Let g_j^2 be the geometric mean at $t_j \in [T^*, T]$.
- Interpolate values $M_j^1 = \log(g_j^1)$ and $M_j^2 = \log(g_j^2)$. Let $\widehat{M^1}(t)$ and $\widehat{M^2}(t)$ be the functions obtained.
- Evaluate the derivative of $\widehat{M^1}(t)$ and $\widehat{M^2}(t)$.
- From Eq. (3.1), obtain the estimate of $C(t)$ and $D(t)$ as follows:
  - For problem 1:
    - Estimation of the model with a therapy affecting only growth rate: $\widehat{C}(t) = \widehat{\alpha} - \frac{d\,\widehat{M^1}(t)}{dt} + \widehat{\beta}\widehat{M^1}(t) + \frac{\widehat{\sigma}^2}{2}, D(t) = 0, \forall t \in [t_0, T]$
    - Estimation of the model with a therapy affecting only death rate: $C(t) = 0, \widehat{D}(t) = \widehat{\beta} - \frac{1}{\widehat{M^1}(t)}\Big[\widehat{\alpha} - \frac{d\,\widehat{M^1}(t)}{dt} - \frac{\widehat{\sigma}^2}{2}\Big], \forall t \in [t_0, T]$
  - For problem 2, we distinguish two situations:
    - If a first therapy mainly affecting cell growth is applied from t_0 up to a time instant $T^* < T$ and a second therapy mainly inducing cell death in $(T^*, T]$ is coupled,

$$\widehat{C}(t) = \widehat{\alpha} - \frac{d\,\widehat{M^1}(t)}{dt} + \widehat{\beta}\widehat{M^1}(t) + \frac{\widehat{\sigma}^2}{2},$$

$$\widehat{D}(t) = \begin{cases} 0 & t \in [t_0, T^*] \\ \widehat{\beta} - \dfrac{1}{\widehat{M^2}(t)}\Big[\widehat{\alpha} - \widehat{C}(t) - \dfrac{d\,\widehat{M^2}(t)}{dt} - \dfrac{\widehat{\sigma}^2}{2}\Big] & t \in (T^*, T] \end{cases}$$

∗ If a therapy mainly inducing cell death is applied from t_0 up to T^* and in $(T^*, T]$ a therapy mainly affecting cell growth is added,

$$\widehat{D}(t) = \widehat{\beta} - \frac{1}{\widehat{M^1}(t)}\Big[\widehat{\alpha} - \frac{d\,\widehat{M^1}(t)}{dt} - \frac{\widehat{\sigma}^2}{2}\Big],$$

$$\widehat{C}(t) = \begin{cases} 0 & t \in [t_0, T^*] \\ \\ \widehat{\alpha} - \dfrac{d\,\widehat{M^2}(t)}{dt} + (\widehat{\beta} - \widehat{D}(t))\widehat{M^2}(t) + \dfrac{\widehat{\sigma}^2}{2}. & t \in (T^*, T]. \end{cases}$$

3.2 Criteria for determining the prevalent effect of a therapy

To determine the prevalent effect of a particular therapy in a preclinical setting in vivo we proposed the strategy of estimating two models (considering $D(t) = 0$ or $C(t) = 0$, $\forall t \in [t_0, T]$), that is

$$\text{Process } X^{(1)}(t): \quad A_1^{(1)}(x,t) = (\alpha - C(t))\,x - \beta\,x\,\ln x \tag{3.2}$$

$$\text{Process } X^{(2)}(t): \quad A_1^{(2)}(x,t) = \alpha\,x - (\beta - D(t))\,x\,\ln x. \tag{3.3}$$

with $A_2(x) = \sigma^2 x^2$ in both cases, and then to choose the one that better fits the observed data. Specifically, in order to determine the prevalent effect of the applied therapy, we establish which distribution (of $X^{(1)}(t)$ or $X^{(2)}(t)$) outperforms the other one in order to fit the sample distribution obtained from the experimental data. To this end, we propose the use of the Kullback-Leibler divergence (KLD), also known as relative entropy, that measures the divergence between two probability distributions. In the case of two continuous distributions with probability density functions f_0 and f_1, the KLD is

$$D_{KL}(f_1||f_0) = \int f_1(x) \log\left(\frac{f_1(x)}{f_0(x)}\right) dx$$

which provides a measure of the information lost when f_0 is used to approximate f_1. In other words, KLD measures how much knowledge of a distribution, e.g. an empirical one, is captured by a proposed one.

In our context, we can use this measure to compute the divergence between the sample distribution (available from the data) and the distributions obtained from each estimated model. The model showing a smaller divergence with respect to the data will be chosen.

Taking into account (2.2), the KLD between the sample and the estimated distributions becomes:

$$D_{KL}(f_s||f_i) = \frac{1}{2}\left[\log\left(\frac{V_i^2(t|\sigma_0^2, t_0)}{V_s^2(t|\sigma_0^2, t_0)}\right) + \frac{V_s^2(t|\sigma_0^2, t_0)}{V_i^2(t|\sigma_0^2, t_0)} + \frac{(M_s(t|\mu_0, t_0) - M_i(t|\mu_0, t_0))^2}{V_i^2(t|\sigma_0^2, t_0)} - 1\right],$$

where the sub-index s refers to the sample distribution, whereas $i = 1, 2$ is associated with the estimated model.

Nevertheless, KLD is not a true distance because it is not a symmetric function and does not satisfy triangular inequality. It is useful nonetheless because of its relation with important statistical concepts such as the log-likelihood ratio. For this reason, many efforts has been made

in order to build distances linked to KLD. One way to do so is through symmetrization. For example, the resistor average distance (see [17])

$$D_{RA}(f_s||f_i) = \frac{D_{KL}(f_s||f_i) \cdot D_{KL}(f_i||f_s)}{D_{KL}(f_s||f_i) + D_{KL}(f_i||f_s)}, \tag{3.4}$$

is a measure based on the harmonic sum of the two possible divergences between two distributions. This distance is applied in several fields. For instance, Neymotin et al. in [24] apply it to the measurement of some characteristics in the context of neuroscience.

In the following sections we will use D_{RA} in order to choose the prevalent effect of a therapy. Functions V_i and M_i will be estimated from (2.3) and (2.4), whereas V_s and M_s will be computing from the data using (2.5) and (2.6), after calculating the arithmetic and geometric means of the sample paths.

In addition, we will consider, for each estimated model, the absolute relative errors

$$Err_{mean} = \frac{1}{N}\sum_{j=1}^{N} \frac{|m_j - \widehat{\mathbb{E}[X^{(i)}(t_j)]}|}{m_j}, \quad Err_{var} = \frac{1}{N^*}\sum_{j=j^*}^{N} \frac{|\sigma_j^2 - \widehat{Var[X^{(i)}}(t_j)]|}{\sigma_j^2} \tag{3.5}$$

where $\widehat{\mathbb{E}[X^{(i)}(t)]}$ and $\widehat{Var[X^{(i)}}(t)]$ are the estimates of $\mathbb{E}[X^{(i)}(t)]$ and $Var[X^{(i)}(t)]$, $i = 1, 2$, and m_j and σ_j^2 are the sample mean and variance at t_j of the sample paths, respectively. Note that for Err_{var}, j^* will be 1 or 2 (and so $N^* = N$ or $N^* = N-1$) depending on the initial distribution being lognormal or degenerate, respectively. These quantities provide a measure of the fit of the models to the data, and they are used as an illustrative example (or preliminary quantification) that there are measurable differences amongst the models, and as such, other, more reliable statistical analyses can be developed to make a more objective and powerful hypothesis testing.

4 Simulation results

The aim of our simulation study is twofold:

1) to compare the actual procedure with the method proposed in [4] for estimating the effect of a single therapy that affects growth rate and

2) to test the validity of the procedure and its ability to select the model underlying the data in order to recognize the nature of the applied therapy in an experimental study.

The control group is described by a Gompertz diffusion process $X(t)$ with infinitesimal moments

$$A_1(x) = \alpha\, x - \beta\, x\, \ln x, \qquad A_2(x) = \sigma^2\, x^2 \qquad (\alpha, \beta, \sigma > 0), \tag{4.1}$$

whereas the treated groups are modeled by means of processes (3.2) and (3.3).

Thus, with models (4.1) and (3.2) we will address our first aim, and with models (4.1), (3.2) and (3.3) we will address the second. Studying the inclusion of a function $D(t)$ in (3.2) once we know function $C(t)$ (that is, the application of a therapy inducing cell death, once estimated the effect of a previous affecting cell growth) would be similar to the comparison between models (3.3) and (4.1). On the other hand, studying the effect of the inclusion of a function $C(t)$ in (3.3) once we know function $D(t)$ (that is, the application of a therapy affecting cell growth, once estimated the effect of a previous inducing cell death) would be similar to the comparative between models (3.2) and (4.1).

In the simulation we have considered several combinations for the parameters of process (4.1), around those used in [4]. Concretely, $\alpha = 0.25, 0.3, 0.35$; $\beta = 0.05, 0.1, 0.15$ and $\sigma = 0.01, 0.02, 0.05$.

For each combination of the parameters, the simulation pattern is as follows: we have simulated 10, 25, and 50 sample paths in the $[0, 50]$ time interval, taking $t_i^* = 0.1(i-1)$, $i = 1, \ldots, 501$, by considering a degenerate initial distribution at 1. After the simulation, we have considered three sample sizes (n=11, 26 and 51 data for each sample path), selecting data equally spaced in the previous time range. Finally, each simulation has been replicated 100 times.

Before tackling any of the two aims of our simulation study we must estimate the parameters of process (4.1). A study has been carried out to find out the influence that the parameter values, the number of paths, and the number of data points selected on each path have on the accuracy of estimations. To this end we have used the absolute relative errors between the real and the estimated values, i.e.:

$$RAE_\alpha = \frac{|\alpha - \widehat{\alpha}|}{\alpha}, \quad RAE_\beta = \frac{|\beta - \widehat{\beta}|}{\beta}, \quad RAE_\sigma = \frac{|\sigma - \widehat{\sigma}|}{\sigma}.$$

In the case of 10 sample paths, Table 1 summarizes the results after applying the estimation procedure developed in [4]. As expected, results on Table 1 indicate that, regardless of the values of α, β, and n, the estimation errors for each parameter increase as σ grows, whereas for fixed values of α and β, errors in σ decrease as n grows.

For the sake of brevity, the others cases (25 and 50 sample paths) are not included, but the conclusions derived from them are similar. The only exception are the errors in the estimation of σ, which logically decrease as more sample information becomes available. Since the accuracy in the estimations of α and β is good and shows little variation, in the following their values will be fixed.

Comparing the procedures for estimating $C(t)$

Model (3.2) was studied in [4] where a procedure for estimating function $C(t)$ was proposed, essentially based on the ratio $\dfrac{\mathbb{E}[X^{(1)}(t)]}{\mathbb{E}[X(t)]}$. Now, the procedure suggested in Section 3 can be used to estimate the same function. In the following we will compare the two procedures when both can be applied.

For this study, two functional forms of the therapy effect (already used in [4]) are considered:

- linear: $C(t) = K\,t$;
- logarithmic: $C(t) = C_0\,\ln(1 + C_1\,t)$.

In both cases the simulation pattern has been the same one used for the control group taking $\alpha = 0.3$, $\beta = 0.1$ with $\sigma = 0.01, 0.02, 0.05$. Concerning the values of the coefficients of the therapeutical functions, we have considered $K = 0.001, 0.002, 0.003$ for the linear therapy, whereas for the logaritmic we have chosen $C_0 = 0.02, 0.03, 0.04$ and $C_1 = 0.15, 0.2, 0.25$.

Table 2 includes, for the case of a linear therapy in which 10 sample paths are taken, the absolute relative errors given by (3.5) (by considering now the theoretical mean and variance functions instead of their sample versions obtained from data) for the selected values of K, σ, and sample size. The results show that both procedures provide similar results regardless of the values of σ and of the sample size. As a matter of fact, the absolute relative errors for the mean and variance functions do not differ much when one or the other procedure is chosen to

			$\alpha = 0.25$			$\alpha = 0.3$			$\alpha = 0.35$		
β	n	σ	RAE_α	RAE_β	RAE_σ	RAE_α	RAE_β	RAE_σ	RAE_α	RAE_β	RAE_σ
0.05	11	0.01	0.00164	0.00240	0.00600	0.00017	0.00010	0.01000	0.00000	0.00000	0.01900
		0.02	0.00264	0.00460	0.01350	0.00053	0.00020	0.01000	0.00049	0.00010	0.02700
		0.05	0.00992	0.01360	0.01480	0.00857	0.01260	0.01120	0.00846	0.01380	0.05200
	26	0.01	0.00164	0.00240	0.00100	0.00100	0.00080	0.00300	0.00003	0.00020	0.01000
		0.02	0.00272	0.00460	0.00750	0.00267	0.00090	0.00700	0.00046	0.00010	0.01050
		0.05	0.01052	0.01460	0.00780	0.00890	0.01180	0.00860	0.00857	0.01400	0.02520
	51	0.01	0.00168	0.00260	0.00100	0.00100	0.00080	0.00000	0.00000	0.00000	0.00600
		0.02	0.00280	0.00480	0.00250	0.00113	0.00090	0.00350	0.00049	0.00010	0.00950
		0.05	0.01056	0.01480	0.00280	0.00997	0.01180	0.00360	0.00857	0.01100	0.00960
0.1	11	0.01	0.00276	0.00340	0.00700	0.00133	0.00140	0.00400	0.00083	0.00140	0.01000
		0.02	0.00304	0.00490	0.01100	0.00137	0.00240	0.01150	0.00137	0.00200	0.01150
		0.05	0.01748	0.02520	0.03260	0.01640	0.02080	0.01520	0.01434	0.01860	0.01960
	26	0.01	0.00284	0.00340	0.00100	0.00097	0.00100	0.00300	0.00069	0.00120	0.00500
		0.02	0.00356	0.00500	0.01100	0.00183	0.00290	0.00600	0.00126	0.00120	0.00550
		0.05	0.01900	0.02710	0.02320	0.01597	0.02060	0.01240	0.01349	0.01790	0.00640
	51	0.01	0.00280	0.00340	0.00000	0.00100	0.00100	0.00200	0.00077	0.00130	0.00300
		0.02	0.00364	0.00520	0.00100	0.00170	0.00280	0.00251	0.00106	0.00190	0.00350
		0.05	0.01988	0.02820	0.00240	0.01653	0.02130	0.01080	0.01391	0.01840	0.00460
0.15	11	0.01	0.00308	0.00373	0.01000	0.00223	0.00220	0.01200	0.00071	0.00150	0.00900
		0.02	0.00572	0.00653	0.01700	0.00517	0.00660	0.00750	0.00343	0.00393	0.01100
		0.05	0.04196	0.04900	0.01240	0.04163	0.04947	0.01080	0.01989	0.02253	0.02100
	26	0.01	0.00292	0.00367	0.00600	0.00153	0.00147	0.00700	0.00063	0.00093	0.00400
		0.02	0.00612	0.00613	0.00650	0.00650	0.00607	0.00550	0.00291	0.00340	0.00750
		0.05	0.04424	0.05193	0.00748	0.04333	0.04913	0.00760	0.01954	0.02267	0.00758
	51	0.01	0.00304	0.00380	0.00100	0.00157	0.00153	0.00600	0.00063	0.00093	0.00100
		0.02	0.00536	0.00740	0.00150	0.00640	0.00793	0.00700	0.00320	0.00373	0.00200
		0.05	0.04496	0.05280	0.00340	0.04317	0.04920	0.00200	0.01977	0.02307	0.00760

Table 1: Absolute relative errors for the estimation of several combinations of the parameters of model (4.1), in the case of 10 sample paths.

approximate function $C(t)$. It can be observed how errors increase with the values of σ, but such increase is similar for both procedures. On the other hand, when the number of paths increases there is a similar trend in errors, which generally decrease at the same rate for both procedures (for the sake of brevity the tables associated with these results have been omitted).

Table 3 shows the case of the logarithmic therapy with a fixed number of paths ($p = 10$) and a fixed number of data points ($n = 11$). The conclusions are similar to those of the linear case, and behave similarly for several numbers of paths and sample sizes.

In order to provide a graphical illustration of some examples, we have selected two of the combinations of the parameters for the therapeutical functions. Concretely, (with $\sigma = 0.01$) we have taken $K = 0.002$ for the linear case and $C_0 = 0.03$, $C_1 = 0.2$ for the logarithmic case (as in [4]). In both cases we have performed a new replication of the simulation with 10 sample paths and we have taken 11 data points for each one. Let $\widehat{C}_{old}(t)$ and $\widehat{C}(t)$ be the estimations of $C(t)$ obtained via the procedure suggested in [4] and in Section 3, respectively. Figure 1(a) includes the results for the linear case. Concretely, the theoretical therapy function (black line), $\widehat{C}_{old}(t)$ (red line) and $\widehat{C}(t)$ (blue line) are shown. In Figure 1(b) the theoretical mean $\mathbb{E}[X^{(1)}(t)]$ (black line) and its estimates obtained by using $\widehat{C}_{old}(t)$ (red line) and $\widehat{C}(t)$ (blue line) are shown. In

K	n	σ	$Err^{(a)}_{mean}$	$Err^{(b)}_{mean}$	$Err^{(a)}_{var}$	$Err^{(b)}_{var}$
0.001	11	0.01	0.00476	0.00504	0.10865	0.10882
		0.02	0.00868	0.00978	0.11800	0.11727
		0.05	0.02198	0.02353	0.12942	0.13279
	26	0.01	0.00463	0.00537	0.08768	0.08762
		0.02	0.00869	0.01025	0.06254	0.06417
		0.05	0.02299	0.02441	0.09444	0.09881
	51	0.01	0.00469	0.00545	0.06138	0.06206
		0.02	0.00886	0.01063	0.04496	0.04737
		0.05	0.02326	0.02506	0.07405	0.08439
0.002	11	0.01	0.00468	0.00515	0.12623	0.12645
		0.02	0.00908	0.01033	0.13324	0.13397
		0.05	0.02436	0.02547	0.10454	0.11265
	26	0.01	0.00475	0.00521	0.06322	0.06384
		0.02	0.00899	0.01056	0.05899	0.06099
		0.05	0.02492	0.02641	0.07091	0.08135
	51	0.01	0.00476	0.00531	0.05792	0.05875
		0.02	0.00978	0.01091	0.04805	0.04990
		0.05	0.02520	0.02639	0.05561	0.06886
0.003	11	0.01	0.00495	0.00522	0.09520	0.09528
		0.02	0.00958	0.01055	0.11860	0.12127
		0.05	0.02396	0.02443	0.13494	0.13788
	26	0.01	0.00530	0.00574	0.06777	0.06804
		0.02	0.00954	0.01090	0.06951	0.07024
		0.05	0.02028	0.02596	0.08468	0.09055
	51	0.01	0.00534	0.00575	0.05461	0.05465
		0.02	0.01005	0.01094	0.05316	0.05628
		0.05	0.02058	0.02660	0.08042	0.08771

Table 2: Absolute relative errors for $X^{(1)}(t)$ with $C(t) = K\,t$, in the case of 10 sample paths. (a) Procedure in [4]; (b) Procedure in Section 3.

Figure 1(c), $Var[X^{(1)}](t)$ (black line) and its estimates obtained by using $\widehat{C}_{old}(t)$ (red line) and $\widehat{C}(t)$ (blue line) are also shown. The results for the logarithmic therapy are shown in Figure 2.

In both cases, the figures illustrate the previous conclusions in the sense that both procedures provide good (the estimated functions are very close to the real ones) and similar results (see the errors in tables 2 and 3 for all replications). However, the procedure suggested in [4] is not able to capture and estimate the effect of a therapy including cell death. Therefore, in the following we will only focus on the procedure proposed in Section 3.

Selection of the data-generating process

The following simulation study aims at testing the validity of the procedure to estimate $C(t)$ or $D(t)$, assuming the other one known, and its ability to select the underlying model for data from a treated group. For this purpose:

- we generate two data sets, each one from the simulation of processes $X^{(1)}(t)$ and $X^{(2)}(t)$;
- for each data set, we estimate two potential models of the type $X^{(1)}(t)$ and $X^{(2)}(t)$;

C_0	C_1	σ	$Err^{(a)}_{mean}$	$Err^{(b)}_{mean}$	$Err^{(a)}_{var}$	$Err^{(b)}_{var}$
0.02	0.15	0.01	0.00485	0.00505	0.11624	0.11635
		0.02	0.00694	0.00962	0.11582	0.11828
		0.05	0.02054	0.02285	0.11222	0.11526
	0.20	0.01	0.00476	0.00521	0.11809	0.11893
		0.02	0.00729	0.00841	0.07888	0.07903
		0.05	0.01997	0.02206	0.12455	0.13193
	0.25	0.01	0.00491	0.00524	0.10734	0.10691
		0.02	0.00912	0.01003	0.13754	0.13820
		0.05	0.01913	0.02197	0.13327	0.13468
0.03	0.15	0.01	0.00399	0.00529	0.11383	0.11361
		0.02	0.00898	0.01042	0.12449	0.12703
		0.05	0.01109	0.01217	0.06138	0.06078
	0.20	0.01	0.00396	0.00537	0.09553	0.09618
		0.02	0.00805	0.00989	0.10760	0.10850
		0.05	0.02091	0.02489	0.12357	0.12855
	0.25	0.01	0.00409	0.00566	0.12123	0.12134
		0.02	0.00854	0.00994	0.11085	0.11169
		0.05	0.01996	0.02385	0.14892	0.15621
0.04	0.15	0.01	0.00461	0.00510	0.13243	0.13265
		0.02	0.00819	0.00851	0.11956	0.11957
		0.05	0.02033	0.02498	0.12288	0.12987
	0.20	0.01	0.00389	0.00458	0.11090	0.11090
		0.02	0.00861	0.00938	0.09236	0.09491
		0.05	0.02104	0.02352	0.10823	0.11416
	0.25	0.01	0.00481	0.00578	0.10629	0.10632
		0.02	0.00974	0.01043	0.14739	0.14891
		0.05	0.02195	0.02252	0.13114	0.13535

Table 3: Absolute relative errors for $X^{(1)}(t)$ with $C(t) = C_0\ \ln(1 + C_1\, t)$, in the case of 10 sample paths and 11 data. (a) Procedure in [4]; (b) Procedure in Section 3.

- we deduce the most appropriate model by comparing the fitted models through the errors made in the estimation of the mean and variance functions and the resistor average distance between the theoretical distribution and that of the models estimated by the proposed methodology.

For this study we assume that the particular processes $X^{(1)}(t)$ and $X^{(2)}(t)$ are characterized by drifts (3.2) and (3.3) with

$$C(t) = C_0\ \ln(1 + C_1\, t), \qquad D(t) = -\frac{r\, t}{\epsilon\, t^2 + 1}. \tag{4.2}$$

respectively. The logarithm function $C(t)$ has been studied by several authors ([4] and [12]) in the study of antitumoral therapies since it seems that this type of therapy is more tolerable than one that linearly increases in time. As regards the function $D(t)$, we have considered a function that produces, at the beginning, a fast increase in the rate of death which will attenuate over time.

For these processes, sample paths have been simulated in the $[0, 50]$ time interval following the same previous simulation pattern by taking $\alpha = 0.3$, $\beta = 0.1$ and considering a range of values

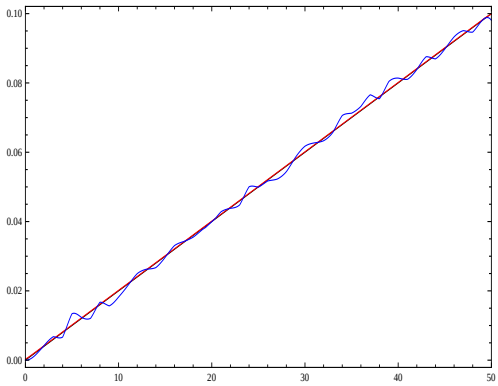

(a) $C(t)$

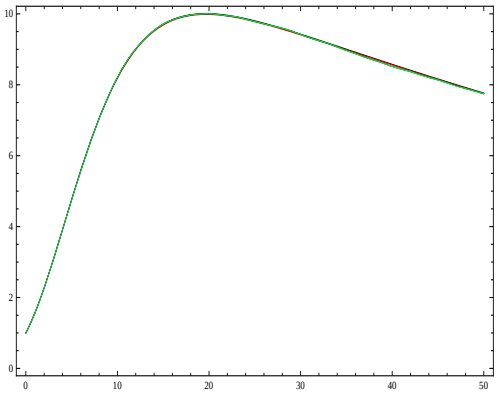

(b) mean

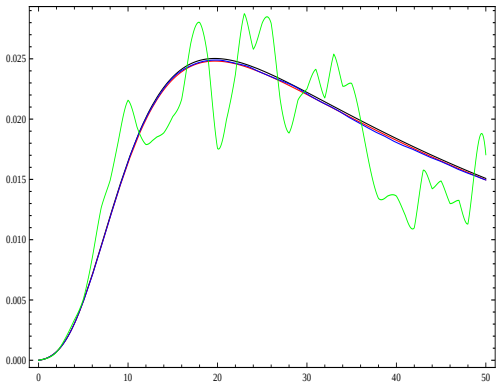

(c) variance

Figure 1: For $C(t) = 0.002\,t$, (a) $C(t)$ (black line), $\widehat{C}_{old}(t)$ (red line) and $\widehat{C}(t)$ (blue line); (b) $\mathbb{E}[X^{(1)}(t)]$ (black line) and its estimates by using $\widehat{C}_{old}(t)$ (red line) and $\widehat{C}(t)$ (blue line); (c) $Var[X^{(1)}](t)$ (black line) and its estimates by using $\widehat{C}_{old}(t)$ (red line) and $\widehat{C}(t)$ (blue line).

for σ and for the coefficients of the therapeutical functions. Concretely, $\sigma = 0.01, 0.02, 0.05$; $C_0 = 0.02, 0.03, 0.04$; $C_1 = 0.15, 0.2, 0.25$; $r = 0.05, 0.1, 0.15$ and $\epsilon = 0.005, 0.01, 0.015$.

Once the models of the type $X^{(1)}(t)$ and $X^{(2)}(t)$ have been fitted, absolute relative errors are calculated for the mean and variance functions of both processes. In order to select the most suitable process using resistor average distance, we have chosen to perform a point-by-point comparison of the distance between the theoretical distribution and that of each of the potential processes estimated. Thus, a measure ($Index$) has been calculated indicating % of times that the distance from the $X^{(1)}(t)$ type process is smaller than that of the $X^{(2)}(t)$ type process. As this index increases, the more suitable becomes the choice of the $X^{(1)}(t)$ type process; as it decreases, the better suited the second model will be. In addition we have calculated the mean difference (in absolute value) between both distances ($DifD_{RA}$). This measurement allows to better distinguish between two situations in which the previous index has the same value. In that case, a greater value for said difference involves a larger discrimination between both fitted

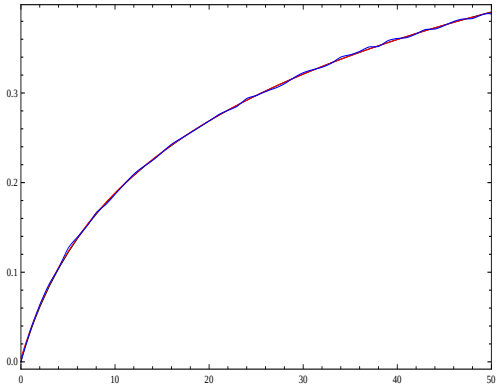

(a) $C(t)$

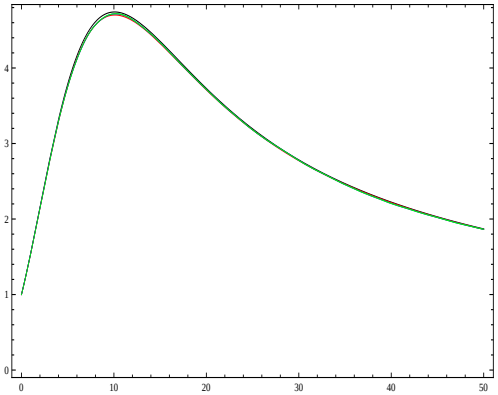

(b) mean

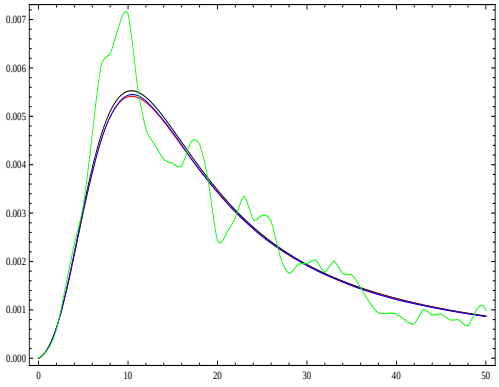

(c) variance

Figure 2: As in Figure 1 with $C(t) = 0.03\,\ln(1 + 0.2\,t)$.

processes.

Table 4 shows the results of the simulation of process $X^{(1)}(t)$, with 10 sample paths and 11 data in each. The values of $Index$ indicate that the procedure performs a correct selection of the model (with values over 70% in all instances). Also, for fixed values of σ and C_0, the increase in the values of C_1 does not affect the differences between the relative errors of the means, although it generates a greater distance between the errors of variances. This also implies that the differences between distances ($DifD_{RA}$) increase, i.e. the procedure performs a better discrimination between the fitted models, and leans towards the first. The same is true when the fixed value is that of C_1. On the other hand, when σ increases so do relative errors, although this does not seem to affect either the index for the selection of the model nor the differences in the distances between models.

We have also verified that the increase in the number of paths and the number of data points in each sample path does not modify the conclusions stated above.

Table 5 is similar to the previous one (with the same number of simulated paths and of data in each) although it simulates process $X^{(2)}(t)$. Results indicate that the procedure also

discriminates correctly (with values of $Index$ below 10%). For fixed values of σ and r, the differences in the errors of means remain mostly invariable as ϵ increases. Nevertheless, said differences decrease in the variances, which implies a decrease in the value of $DifD_{RA}$. Therefore, the lower ϵ becomes, the better the discrimination between the models. When the fixed value is that of ϵ the general trend is the reverse to the previously stated, as r increases.

Again, the increase in the number of paths and in the number of data points for each does not modify the conclusions above.

C_0	C_1	σ	$Err^{(a)}_{mean}$	$Err^{(b)}_{mean}$	$Err^{(a)}_{var}$	$Err^{(b)}_{var}$	$Index$	$DifD_{RA}$
0.02	0.15	0.01	0.00384	0.00436	0.03516	0.04466	100	0.00314
		0.02	0.00768	0.00772	0.21630	0.29123	100	0.00914
		0.05	0.01512	0.01600	0.06790	0.08691	80	0.00111
	0.20	0.01	0.00426	0.00448	0.05183	0.07726	90	0.00431
		0.02	0.00492	0.00531	0.22393	0.31029	100	0.01114
		0.05	0.02380	0.02328	0.10870	0.14244	80	0.00219
	0.25	0.01	0.00573	0.00616	0.05761	0.08312	100	0.00885
		0.02	0.00631	0.00683	0.22896	0.32507	100	0.01380
		0.05	0.04471	0.04280	0.17657	0.26374	70	0.00210
0.03	0.15	0.01	0.00481	0.00535	0.05964	0.09904	100	0.00746
		0.02	0.01130	0.01127	0.22275	0.33573	100	0.01633
		0.05	0.01430	0.01455	0.09612	0.17185	100	0.00179
	0.20	0.01	0.00587	0.00615	0.04941	0.13069	90	0.01103
		0.02	0.00421	0.00468	0.22776	0.35681	100	0.01875
		0.05	0.02247	0.02360	0.05138	0.15396	100	0.00460
	0.25	0.01	0.00352	0.00397	0.05845	0.13998	80	0.01683
		0.02	0.00542	0.00571	0.23035	0.37225	100	0.02137
		0.05	0.04217	0.04187	0.06468	0.15180	100	0.00793
0.04	0.15	0.01	0.00410	0.00487	0.06341	0.14256	100	0.01264
		0.02	0.00600	0.00623	0.23066	0.37847	100	0.02192
		0.05	0.01427	0.01459	0.06269	0.15302	90	0.00500
	0.20	0.01	0.00387	0.00532	0.05778	0.17543	100	0.02517
		0.02	0.01383	0.01450	0.20383	0.37619	100	0.03258
		0.05	0.01418	0.01576	0.04858	0.20220	100	0.00794
	0.25	0.01	0.00365	0.00494	0.06224	0.19671	100	0.02745
		0.02	0.00801	0.00855	0.21664	0.40747	100	0.03573
		0.05	0.01773	0.01870	0.07625	0.19649	90	0.01139

Table 4: Absolute relative errors and index for choosing the model that best fits the data. Data generated by process $X^{(1)}(t)$, in the case of 10 sample paths and 11 data points. Estimated model: (a) type $X^{(1)}(t)$; (b) type $X^{(2)}(t)$.

As in the study that compared the estimation procedures of $C(t)$, we will now illustrate some particular cases. Specifically, we will consider $C(t) = 0.03\log(1 + 0.2t)$ when simulating a process of the type $X^{(1)}(t)$, and $D(t) = -0.1/(0.01t^2 + 1)$ when the process is of the type $X^{(2)}(t)$. In both cases we have simulated 10 sample paths taking $\sigma = 0.01$ and then considering 11 data points for each one.

The sample paths of $X(t)$ (control group) and of $X^{(1)}(t)$, which models the group treated with the therapy affecting cell growth $C(t)$, are shown in Figure 3(a). Similarly, Figure 3(b) shows the sample paths of $X(t)$ and of $X^{(2)}(t)$ modeling the group treated with the therapy inducing cell death $D(t)$.

r	ϵ	σ	$Err^{(a)}_{mean}$	$Err^{(b)}_{mean}$	$Err^{(a)}_{var}$	$Err^{(b)}_{var}$	$Index$	$DifD_{RA}$
0.05	0.005	0.01	0.01101	0.00276	2.60568	0.06325	0	0.67915
		0.02	0.01296	0.00623	1.65285	0.21591	10	0.25703
		0.05	0.01338	0.00923	2.72032	0.06640	0	0.20885
	0.010	0.01	0.00872	0.00323	1.60824	0.06105	0	0.32063
		0.02	0.00901	0.00502	0.91320	0.22200	0	0.10432
		0.05	0.01978	0.01596	1.71586	0.10403	0	0.12082
	0.015	0.01	0.00676	0.00501	1.21567	0.06793	0	0.10910
		0.02	0.00761	0.00680	0.61671	0.21991	20	0.04688
		0.05	0.02509	0.02593	1.39038	0.15638	10	0.07018
0.10	0.005	0.01	0.00586	0.00795	5.34749	0.08495	10	0.44391
		0.02	0.00903	0.00919	3.67151	0.20864	10	0.31447
		0.05	0.01184	0.01283	5.57470	0.11286	10	0.40730
	0.010	0.01	0.00573	0.00948	3.29242	0.08815	10	0.25033
		0.02	0.00490	0.00899	2.12893	0.20668	10	0.14515
		0.05	0.01018	0.01392	3.36682	0.08181	10	0.25740
	0.015	0.01	0.00686	0.00891	2.46270	0.08910	10	0.21658
		0.02	0.00714	0.00983	1.52388	0.20324	10	0.10652
		0.05	0.02181	0.02414	2.62420	0.15222	10	0.16690
0.15	0.005	0.01	0.01789	0.01106	8.31349	0.11037	10	0.96902
		0.02	0.02009	0.01194	5.82685	0.21411	10	0.57323
		0.05	0.02310	0.02096	8.52895	0.14999	10	0.53733
	0.010	0.01	0.01791	0.00915	5.13505	0.10194	10	0.82830
		0.02	0.02220	0.01136	3.51572	0.20655	10	0.41498
		0.05	0.01985	0.01311	5.20792	0.10457	10	0.37876
	0.015	0.01	0.01974	0.00973	3.83176	0.10030	10	0.72281
		0.02	0.02122	0.01135	2.54057	0.20792	10	0.31557
		0.05	0.02377	0.01232	3.93798	0.10183	10	0.29474

Table 5: Absolute relative errors and index for choosing the model that best fits the data. Data generated by process $X^{(2)}(t)$, in the case of 10 sample paths and 11 data points. Estimated model: (a) type $X^{(1)}(t)$; (b) type $X^{(2)}(t)$.

We first use the data obtained by the simulation of process $X^{(1)}(t)$, and then estimate models (3.2) and (3.3). Clearly, the estimate of (3.2) will provide the estimate of $C(t)$ assuming that $D(t) = 0$, whereas the estimate of (3.3) will assume $C(t) = 0$ and will provide the estimate of $D(t)$. In Figure 4 this case is illustrated. Figure 4(a) shows the theoretical $C(t)$ (black line) and its estimate found by using model $X^{(1)}(t)$ (red curve). The blue straight line indicates zero, which is the estimate of $C(t)$ provided by model $X^{(2)}(t)$. In Figure 4(b) the theoretical mean $\mathbb{E}[X^{(1)}(t)]$ (black line) and its estimates found by using $X^{(1)}(t)$ (red line) and $X^{(2)}(t)$ (blue line) are shown. Both of them appear to be very close to $\mathbb{E}[X^{(1)}(t)]$. On the other hand, the estimates of variance $Var[X^{(1)}(t)]$ provide different results, as shown in Figure 4(c). As a matter of fact, the estimated variance found by using the wrong model $X^{(2)}(t)$ (blue line) appears to be far from the theoretical $Var[X^{(1)}](t)]$ (black line), showing that model $X^{(1)}$ is more appropriate for these data. This is also evident in Figure 4(d), in which the D_{RA} distance given by (3.4) between the theoretical model and the estimated of type $X^{(1)}(t)$ is closer to zero, at each time instant, than the distance found when a process of the type $X^{(2)}(t)$ is considered (blue line).
Figure 5 shows the results from the data obtained by process $X^{(2)}(t)$. Figure 5(a) shows the theoretical $D(t)$ (black line) and its estimate by using model $X^{(2)}(t)$ (blue curve). The red

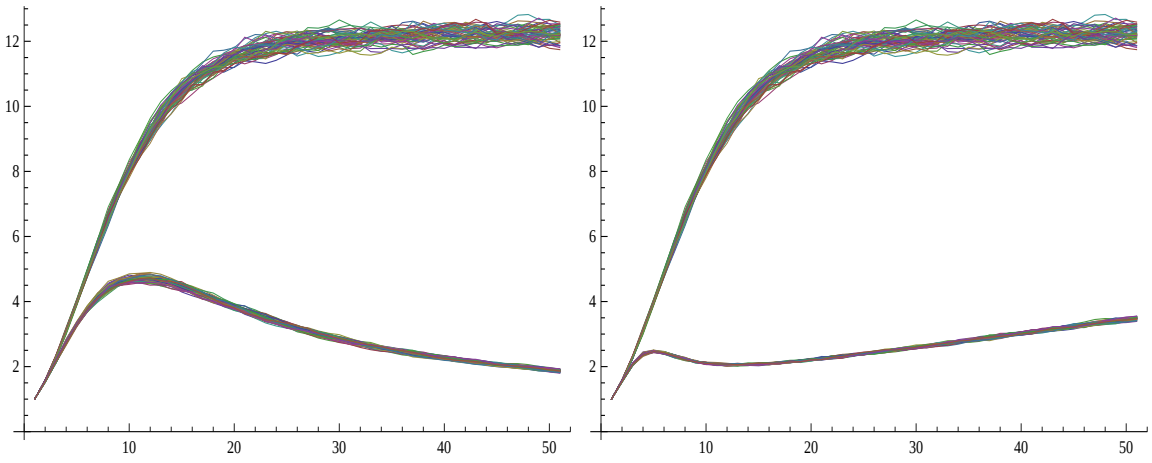

Figure 3: (a) Simulated sample paths of $X(t)$ (top) and of $X^{(1)}(t)$ (bottom) with $C(t) = 0.03\log(1 + 0.2t)$; (b) Simulated sample paths of $X(t)$ (top) and of $X^{(2)}(t)$ (bottom) with $D(t) = -0.1/(0.01t^2 + 1)$.

straight line indicates zero, which is the estimate of $D(t)$ provided by model $X^{(1)}(t)$. In this case the mean seems to not be able to discriminate the right underlying process (see Figure 5(b)), while the estimated variance (see Figure 5(c)) from the model $X^{(1)}(t)$ (red line) detects a problem to fit the theoretical variance (black line). Finally, the D_{RA} distance is confirmed to be a useful instrument to select the right underlying model. In this case (see Figure 5(d)) the D_{RA} distance of the estimated process of the type $X^{(2)}(t)$ with respect to the theoretical distribution (blue line) fluctuates near zero.

5 Application to real data

In this section we consider an application of the methodology introduced in this paper to experimental data obtained in mice engrafted with patient-derived uveal melanoma tumors (patient-derived xenografts) and treated with different therapeutic agents (certican, dasatinib, and avastin). Our goal was to check if this method is able to correctly determine the predominant mechanism of action (growth versus death rate).

Whereas certican has been reported to display a cytostatic activity in several in vitro and in vivo tumor models ([11], [16], [34], [35]), dasatinib exerts its anti-tumor activity at least partially by induction of apoptosis ([22], [31]). Avastin has been demonstrated to reduce tumor growth without inducing apoptosis in several models ([23], [29]) but apoptosis has been evidenced in patients with inflammatory breast cancer ([33]). This indicates that in some cases in vitro data are not relevant. The mechanism of action of avastin needs to be adressed in vivo, given that this drug avastin could indirectly affect tumor cell growth by affecting endothelial cells.

We will focus on the first problem discussed in Section 2: to determine for each therapy applied its effect on tumor cells (growth versus death rate) or, at least, to deduce its prevalent effect. We will demonstrate that our methodology confirms the already reported prevalent growth inhibition effect of certican and the predominant apoptotic activity of dasatinib. These results suggest that this methodology could be useful to get insights into the mechanism of actions displayed by drugs in vivo. In this way the data obtained with avastin allows to deduce

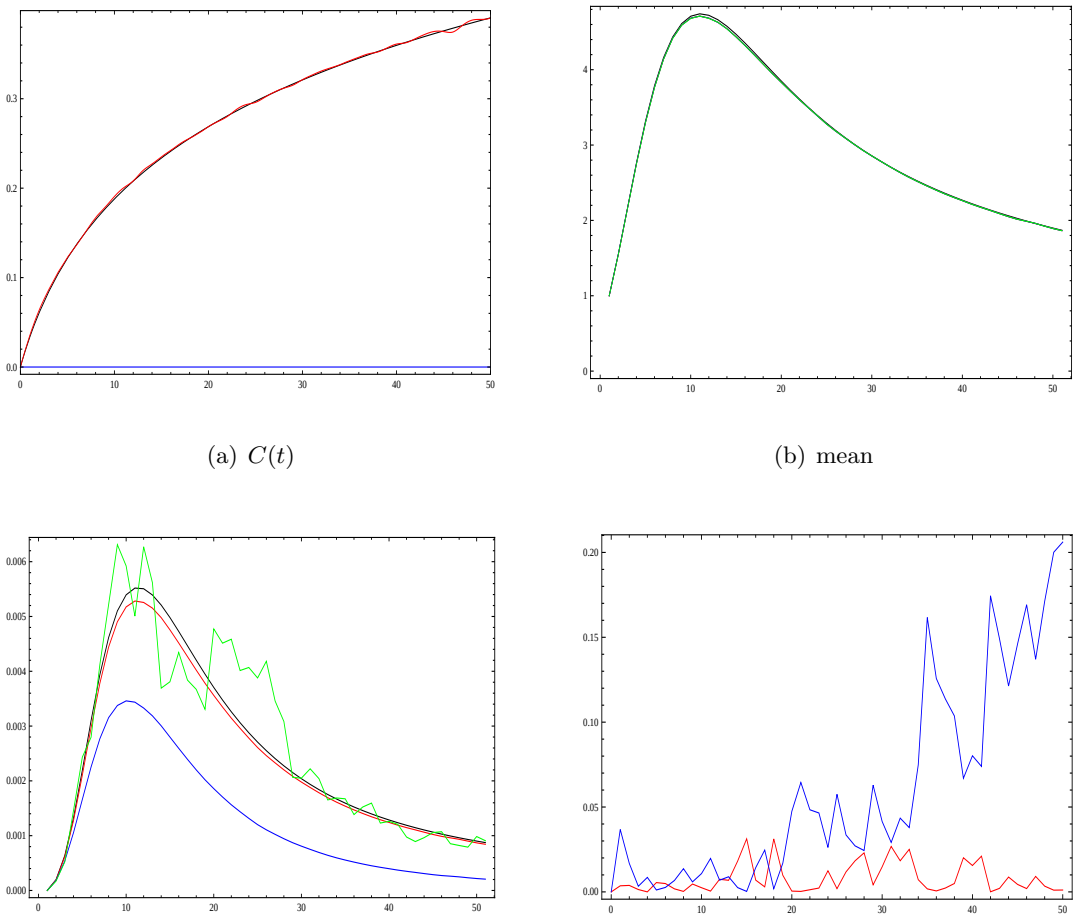

(a) $C(t)$ (b) mean

(c) variance (d) D_{RA} distance

Figure 4: For data generated by process $X^{(1)}(t)$, (a) $C(t)$ (black line), $\widehat{C}(t)$ (red line) obtained via model (3.2); (b) $\mathbb{E}[X^{(1)}(t)]$ (black line) and its estimates by using $X^{(1)}(t)$ (red line) and $X^{(2)}(t)$ (blue line); (c) $Var[X^{(1)}(t)]$ (black line) and its estimates by using $X^{(1)}(t)$ (red line) and $X^{(2)}(t)$ (blue line); (d) D_{RA} distance between the distribution of $X^{(1)}(t)$ and the theoretical distribution (red line) and D_{RA} distance between the distribution of $X^{(2)}(t)$ and the theoretical distribution (blue line).

a predominant effect on growth rate.

We have considered data about the growth of MP55BL tumor from four experimental groups of 8, 5, 8 and 7 mice, respectively. The first is the untreated group (control). The other three groups of mice were treated with dasatinib (per os, 50mg/Kg, 5 days a week), certican (per os, 2mg/Kg, 3 days a week) and avastin (intraperitoneally, 30mg/Kg, once a week), respectively. The tumor volume was measured at days 1, 5, 9, 13, 17, 19, 22, and 26, and the relative volume of tumor with respect to the initial volume was calculated. Figure 6 shows the mean of the relative tumor volume for the four experimental groups as a function of the days after starting the treatment.

From the data of the control group, the estimated parameters of the Gompertz diffusion process (4.1) are

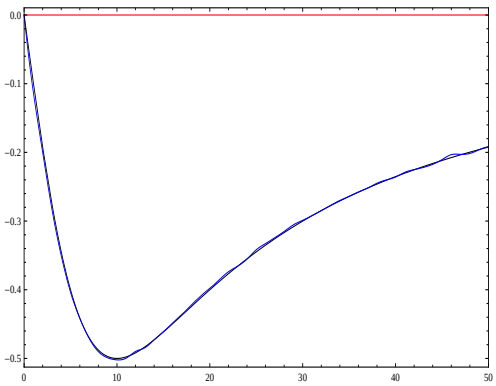

(a) $D(t)$

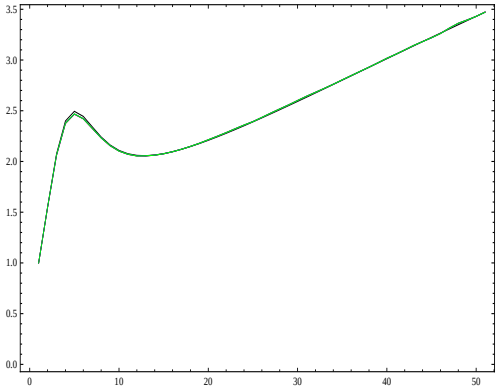

(b) mean

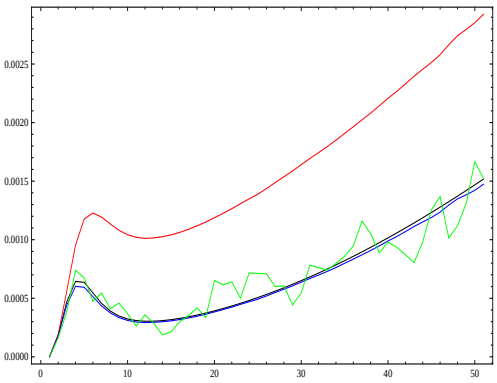

(c) variance

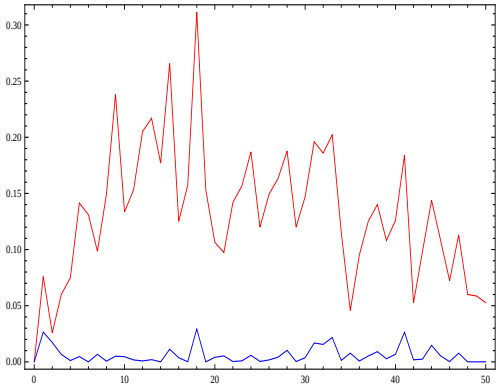

(d) D_{RA} distance

Figure 5: As in Figure 4, when data are generated by $X^{(2)}(t)$.

$$\widehat{\alpha} = 0.0826194, \qquad \widehat{\beta} = 0.0028546, \qquad \widehat{\sigma} = 0.0589.$$

To determine the nature (or, at least, the prevalent effect) of each applied therapy, for each treated group we have estimate models of type (3.2) and (3.3). Table 6 shows the absolute relative errors for each treated group with respect to each estimated model.

Table 6: Absolute relative errors for the mean and variance functions

	Dasatinib treated group		Certican treated group		Avastin treated group	
	$X^{(1)}(t)$	$X^{(2)}(t)$	$X^{(1)}(t)$	$X^{(2)}(t)$	$X^{(1)}(t)$	$X^{(2)}(t)$
Err_{mean}	0.08379	0.04439	0.07355	0.06887	0.04501	0.03871
Err_{var}	0.46932	0.31577	0.57431	0.70256	0.28978	0.81475

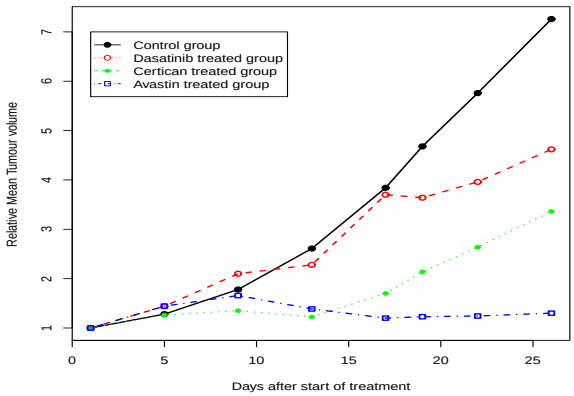

Figure 6: Tumor growth for the four experimental groups.

In all cases, from the differences between the errors associated with the mean we cannot deduce the most appropriate model. From the information provided by the errors associated with the variance it seems that the most appropriate models are of the type $X^{(2)}(t)$ for the dasatinib treated group, and of the type $X^{(1)}(t)$ for the certican and avastin treated groups. However this criterion is not too clear.

Figures 7, 8 and 9 show the D_{RA} distances between the dasatinib, certican, and avastin treated groups and their corresponding estimated models of the type $X^{(1)}(t)$ and $X^{(2)}(t)$.

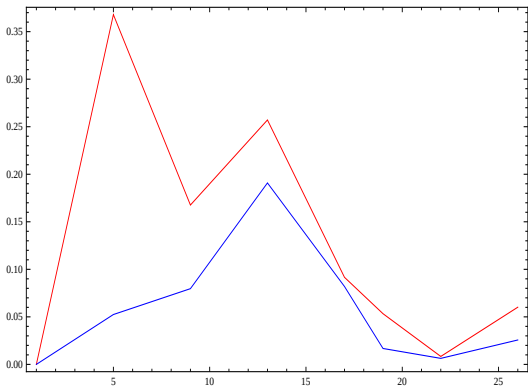

Figure 7: D_{RA} distances to model $X^{(1)}(t)$ (red line) and to model $X^{(2)}(t)$ (blue line) for the dasatinib treated group.

From this information, we can more clearly confirm the conclusions drawn from the errors associated with the variance.

Our application classifies certican as a modulator of growth rate and dasatinib as a modulator of cell death. These results are in accord with in-vitro data showing a cytostatic effect of certican on uveal melanoma cell lines and an induction of cell death by dasatinib in these cells. Avastin can modulate tumor dynamics by directly inhibiting tumor cell proliferation or indirectly by affecting angiogenesis. Our data suggest that in our tumor model avastin affects predominantly tumor cell proliferation with a similar pattern to that observed with certican.

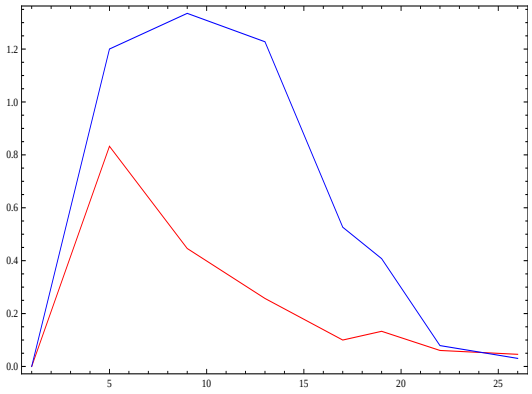

Figure 8: D_{RA} distances to model $X^{(1)}(t)$ (red line) and to model $X^{(2)}(t)$ (blue line) for the certican treated group.

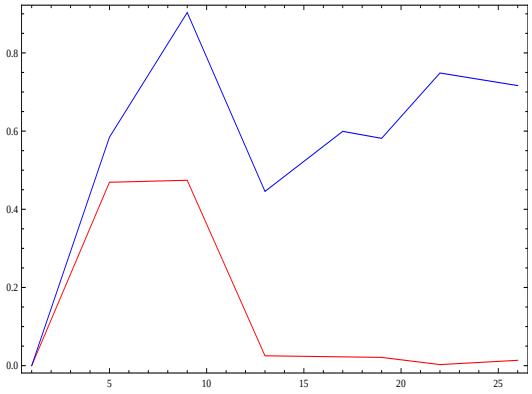

Figure 9: D_{RA} distances to model $X^{(1)}(t)$ (red line) and to model $X^{(2)}(t)$ (blue line) for the avastin treated group.

Once this methodology has been applied to detect the kind of effect displayed by the different drugs, the analysis of the estimations of the corresponding functions $C(t)$ and $D(t)$ could hopefully allow to obtain some information about the influence of therapeutic schedules on tumor growth kinetics. Figures 10 and 11 show the functions that model the effect therapy ($D(t)$ for the model of type $X^{(2)}(t)$ in the dasatinib treated group and $C(t)$ for models of type $X^{(1)}(t)$ in the certican and avastin treated groups).

As depicted in Figure 10, treatment with dasatinib results in a deceleration of tumor growth rate only after one week of treatment and after an acceleration of the growth rate during the first week. This is followed by an alternance of acceleration/deceleration periods in which accelerations are significantly less and less pronounced. At the end of the treatment deceleration prevails over acceleration of tumor growth rate.

Treatment with certican (see Figure 11) resulted in a reduction in growth rate over the time of treatment with the exception of the third week, in which a transient weak increase of growth rate was observed. In fact a decrease of the tumor size was found during the second week of treatment. After 21 days the effect of certican on the decrease of growth rate was weaker than

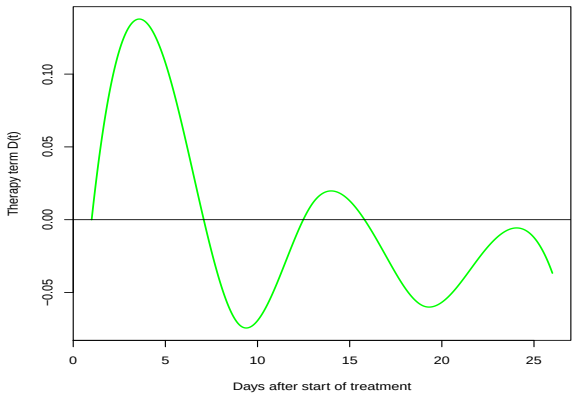

Figure 10: Estimated $D(t)$ function of a model of type $X^{(2)}(t)$ for the dasatinib treated group.

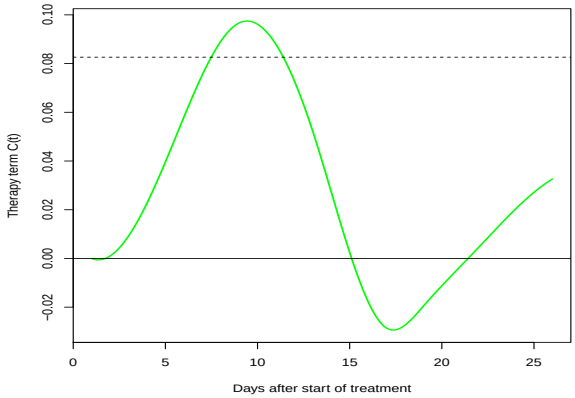

Figure 11: Estimated $C(t)$ functions of a model of type $X^{(1)}(t)$ for the certican and avastin treated groups. Dashed line represents the value of α.

that observed at the beginning of the treatment.

Treatment with avastin (see Figure 11) resulted in a decrease of tumor growth rate throughout the entire treatment period. A very significant reduction in the tumor size takes place between days 9 and 17 and an almost imperceptible reduction between days 22 and 24.

$C(t)$ estimations for both certican and avastin (two drugs affecting tumor growth rate rather than tumor death rate) have been depicted in the same figure (Figure 11) in order to properly compare the effects of therapy on tumor behavior in mice. It can be observed that these two drugs perform similarly in the first three or four days, then certican performs better than avastin until day 9. However, after 9 days of treatment avastin becomes more efficient than certican and it remains more performant until the end of the experiment. We can also observe periods of tumor regression with both agents. A regression period could be obtained earlier with certican than with avastin, but the magnitude of that obtained with avastin was significantly higher. A second smaller tumor regression period could be detected only with avastin. Therefore, representation of functions that model the effect of therapies can help to more accurately analyse the kinetics of anticancer drugs in vivo and also could help to propose hypothesis about the mechanism of

action displayed by drugs in an in-vivo preclinical setting.

Concluding remarks

A modified Gompertz diffusion process including exogenous factors in its infinitesimal mean has been considered here in order to model the effect of anti-proliferative and/or pro-apoptotic therapies. A procedure to estimate the time dependent functions representing the effect of a therapy assuming that one of the functions is known, has been proposed. This is the case when therapies are assessed in combination and experimental data of a control untreated group, and of groups treated with single and combined therapies, are available. A comparison has been made between the actual procedure and the method proposed in [4] to estimate the effect of an anti-proliferative therapy.

A criterion to deduce the nature of the anti-tumor effect (reduction of growth rate or increase of death rate) for each applied drug, or at least its prevalent effect, has been proposed. This criterion is essentially based on the Kullback Leibler divergence between the distribution of the estimated models and the sample distribution.

We have applied our criterion to real data obtained from uveal melanoma xenografts challenged with different therapies displaying different mechanisms of action. Importantly, the results obtained fit with the mechanism of action observed in vitro with tumor cells, and suggest that our method can be successfully applied to get insights into the mechanism of action displayed by a given drug or drug combination in vivo.

Moreover, the estimation of functions that model the effect of therapies allows us to analyse the kinetics of anticancer drugs in vivo.

Acknowledgements

The authors are very grateful to Dr Fariba Nemati and Dr Didier Decaudin at Translational Research Department of Institut Curie, Paris, for providing the data used in this research, and to the anonymous referees whose comments and suggestions have contributed to improve this paper.
This work was supported in part by the Ministerio de Economía y Competitividad, Spain, under Grant MTM2011-28962 and by University of Salerno grant program "Sistema di calcolo ad alte prestazioni per l'analisi economica, finanziaria e statistica (High Performance Computing - HPC)- prot. ASSA098434, 2009.

References

[1] Arnold, L., 1974. Stochastic Differential Equations. Wiley, NewYork.

[2] Albano, G., Giorno, V., 2006. A stochastic model in tumor growth. J. Theor. Biol. 242, 329-336.

[3] Albano, G., Giorno, V., Saturnino, C., 2007. A prey-predator model for immune response and drug resistance in tumor growth. In Computer Aided Systems Theory EUROCAST 2007 (Moreno-Diaz R.,Pichler F.R. and Quesada-Arencibia A., eds.) Lect. Notes Comput. Sc. 4739, 171-178.

[4] Albano, G., Giorno, V., Román-Román, P., Torres-Ruiz, F., 2011. Inferring the effect of therapy on tumors showing stochastic Gompertzian growth. J. Theor. Biol. 276, 67-77.

[5] Albano, G., Giorno, V., Román-Román, P., Torres-Ruiz, F., 2012. Inference on a stochastic two-compartment model in tumor growth. Comput. Stat. Data An. 56, 1723-1736.

[6] Albano, G., Giorno, V., Román-Román, P., Torres-Ruiz, F., 2013. On the effect of a therapy able to modify both the growth rates in a Gompertz stochastic model. Math. Biosci. 245, 12-21.

[7] Bachelot, T., Bourgier, C., Cropet, C., Ray-Coquard, I., Ferrero, J.M., Freyer, G., Abadie-Lacourtoisie, S., Eymard, J.C., Debled, M., Spaëth, D., Legouffe, E., Allouache, D., El Kouri, C., Pujade-Lauraine, E., 2012. Randomized phase II trial of everolimus in combination with tamoxifen in patients with hormone receptor-positive, human epidermal growth factor receptor 2-negative metastatic breast cancer with prior exposure to aromatase inhibitors: a GINECO study. J. Clin. Oncol. 30, 2718-2724.

[8] Baselga, J., Corts, J., Kim, S.B., Im, S.A., Hegg, R., Im, Y.H., Roman, L., Pedrini, J.L., Pienkowski, T., Knott, A., Clark, E., Benyunes, M.C., Ross, G., Swain, S.M., 2012. Pertuzumab plus trastuzumab plus docetaxel for metastatic breast cancer. N. Engl. J. Med. 366, 109-119.

[9] Cameron, D.A., Ritchie, A.A., Langdon, S., Anderson, T.J., Miller, W.R., 1997. Tamoxifen induced apoptosis in ZR-75 breast cancer xenografts antedates tumor regression. Breast Cancer Res. Tr. 45, 99-107.

[10] Cameron, D.A., Ritchie, A.A., Miller, W.R., 2001. The relative importance of proliferation and cell death in breast cancer growth and response to tamoxifen. Eur. J. Cancer 37, 1545-1553.

[11] Chan, S.L., Wong, C.H., Lau, C.P., Zhou, Q., Hui, C.W., Lui, V.W., Ma, B.B., Chan, A.T., Yeo, W., 2013. Preclinical evaluation of combined TKI-258 and RAD001 in hepatocellular carcinoma. Cancer Chemother. Pharmacol., 71(6): 1417-1425.

[12] de Vladar, H.P., Gonzalez, J.A., Rebolledo, M., 2003. New-late intensification schedules for cancer treatments. Acta Cient. Venez. 54, 263-276.

[13] de Vladar, H.P., Gonzalez, J.A., 2004. Dynamic response of cancer under the influence of immunological activity and therapy. J. Theor. Biol. 227, 335-348.

[14] Flaherty, K.T., Infante, J.R., Daud, A., Gonzalez, R., Kefford, R.F., Sosman, J., Hamid, O., Schuchter, L., Cebon, J., Ibrahim, N., Kudchadkar, R., Burris, H.A., Falchook, G., Algazi, A., Lewis, K., Long, G.V., Puzanov, I., Lebowitz, P., Singh, A., Little, S., Sun, P., Allred, A., Ouellet, D., Kim, K.B., Patel, K., Jeffrey Weber, J., 2012. Combined BRAF and MEK Inhibition in Melanoma with BRAF V600 Mutations. N. Engl. J. Med. 367, 1694-1703.

[15] Gerlee, P. 2013. The Model Muddle: In Search of Tumor Growth Laws. Cancer Res. 73, 2407-2411.

[16] Janes, M.R., Vu, C., Mallya, S., Shieh, M.P., Limon, J.J., Li, L.S., Jessen, K.A., Martin, M.B., Ren, P., Lilly. M.B., Sender, L.S., Liu, Y., Rommel. C., Fruman. D.A., 2013. Efficacy of the investigational mTOR kinase inhibitor MLN0128/INK128 in models of B-cell acute lymphoblastic leukemia. Leukemia, 27(3): 586-594.

[17] Johnson, D.H., Sinanovic, S., 2001. Symmetrizing the Kullback-Leibler distance. Available at http://www.ece.rice.edu/∼dhj/resistor.pdf.

[18] Giorno, V., Spina, S. (2013) A jump stochastic Gompertz model for an intermittent treatment in tumor growth. Lecture Notes in Computer Science, Vol. 8111. Springer-Verlag, Berlin, 61-68.

[19] Hirata, Y., Bruchovsky, N., Aihara, K., 2010. Development of a mathematical model that predicts the outcome of hormone therapy for prostate cancer. J. Theor. Biol. 264, 517-527.

[20] Lo, C.F., 2007. Stochastic Gompertz model of tumor cell growth. J. Theor. Biol. 248, 317-321.

[21] Lo, C.F., 2010. A modified stochastic Gompertz model for tumor cell growth. Comp. Math.Meth. Med. 11(1), 3-11.

[22] Michels, S., Trautmann, M., Sievers, E., Kindler, D., Huss, S., Renner, M., Friedrichs, N., Kirfel, J., Steiner, S., Endl, E., Wurst, P., Heukamp, L., Penzel, R., Larsson, O., Kawai, A., Tanaka, S., Sonobe, H., Schirmacher, P., Mechtersheimer, G., Wardelmann, E., Bttner, R., Hartmann, W., 2013. SRC signaling is crucial in the growth of synovial sarcoma cells. Cancer Res., 73(8): 2518-2528

[23] Michishita, M., Uto, T., Nakazawa, R., Yoshimura, H., Ogihara, K., Naya, Y., Tajima, T., Azakami, D., Kishikawa, S., Arai, T., Takahashi, K., 2013. Antitumor effect of bevacizumab in a xenograft model of canine hemangiopericytoma. J. Pharmacol. Sci., 121(4): 339-342.

[24] Neymotin, S.A., Lytton, W.W., Olypher, A.V. and Fenton, A.A., 2011. Measuring the quality of neuronal identification in ensemble recordings. J. Neurosci., 31(45), 16398-16409.

[25] Norton, L., 1988. A Gompertzian Model of Human Breast Cancer Growth. Cancer Res. 48, 7067-7071.

[26] Nobile, A.G., Ricciardi, L.M., 1980. Growth and extinction in random environment. In: Advances in Communication. Vol. 3: Application of Information and Control Systems (Lainiotis, D.G. and Tzannes, N.S. eds.), 455-465.

[27] Parfitt, A. M., Fyhrie, D.P., 1997. Gompertzian growth curves in parathyroid tumours: further evidence for the set-point hypothesis. Cell Proliferat. 30, 341-349.

[28] Prahallad, A., Sun, C., Huang, S., Di Nicolantonio, F., Salazar, R., Zecchin, D., Beijersbergen, R.L., Bardelli, A., Bernards, R., 2012. Unresponsiveness of colon cancer to BRAF(V600E) inhibition through feedback activation of EGFR. Nature 482, 100-103.

[29] Rapisarda, A., Hollingshead, M., Uranchimeg, B., Bonomi, C.A., Borgel, S.D., Carter, J.P., Gehrs, B., Raffeld, M., Kinders, R.J., Parchment, R., Anver, M.R., Shoemaker, R.H., Melillo, G., 2009. Increased antitumor activity of bevacizumab in combination with hypoxia inducible factor-1 inhibition. Mol. Cancer Ther., 8(7): 1867-1877

[30] Román-Román, P., Torres-Ruiz, F., 2012. Inferring the effect of therapies on tumor growth by using diffusion processes. J. Theor. Biol. 314, 34-56.

[31] Simara, P., Stejskal, S., Koutna, I., Potesil, D., Tesarova, L., Potesilova, M., Zdrahal, Z., Mayer, J., 2013. Apoptosis in chronic myeloid leukemia cells transiently treated with imatinib or dasatinib is caused by residual BCR-ABL kinase inhibition. Am. J. Hematol, 88(5): 385-393

[32] Stepanova, N., 1980. Course of the immune reaction during the development of a malignant tumor. Biophysics 24, 917-923.

[33] Wedam, S.B., Low, J.A., Yang, S.X., Chow, C.K., Choyke, P., Danforth, D., Hewitt, S.M., Berman, A., Steinberg, S.M., Liewehr, D.J., Plehn, J., Doshi, A., Thomasson, D., McCarthy, N., Koeppen, H., Sherman, M., Zujewski, J., Camphausen, K., Chen, H., Swain, S.M., 2006. Antiangiogenic and antitumor effects of bevacizumab in patients with inflammatory and locally advanced breast cancer. J. Clin. Oncol., 24(5): 769-777.

[34] Weigelt B., Warne P.H., Downward J., 2011. PIK3CA mutation, but not PTEN loss of function, determines the sensitivity of breast cancer cells to mTOR inhibitory drugs. Oncogene, 30(29):3222-3233.

[35] Weiler, M., Pfenning, P.N., Thiepold, A.L., Blaes, J., Jestaedt, L., Gronych, J., Dittmann, L.M,, Berger, B., Jugold, M., Kosch, M., Combs, S.E., von Deimling, A., Weller, M., Bendszus, M., Platten, M., Wick, W., 2013. Suppression of proinvasive RGS4 by mTOR inhibition optimizes glioma treatment. Oncogene, 32(9):1099-1109.

A Appendix. Distribution of the process

To find the solution of (2.1) we set

$$Z(t) = \frac{k(t)}{\sigma}\,\ln X(t), \tag{A.1}$$

where $k(t) = \exp\left\{\beta(t-t_0) - \int_{t_0}^{t} D(\theta)\,d\theta\right\}$. Making use of (A.1), by Ito's lemma, equation (2.1) becomes

$$d\,Z(t) = \frac{k(t)}{\sigma}\left[\alpha - C(t) - \frac{\sigma^2}{2}\right]dt + k(t)\,d\,W(t), \qquad Z(t_0) = Z_0 = \frac{k(t_0)}{\sigma}\,\ln X_0. \tag{A.2}$$

Note that (A.2) is a linear stochastic differential equation, whose solution is

$$Z(t) = Z_0 + \frac{1}{\sigma}\int_{t_0}^{t} k(\theta)\left[\alpha - C(\theta) - \frac{\sigma^2}{2}\right]d\theta + \int_{t_0}^{t} k(\theta)\,dW(\theta) \tag{A.3}$$

Recalling (A.1), from (A.3) one can obtain the solution of (2.1):

$$X(t) = \exp\left\{\frac{k(t_0)}{k(t)}\ln X_0 + \frac{1}{k(t)}\int_{t_0}^{t}\left[\alpha - C(\theta) - \frac{\sigma^2}{2}\right]k(\theta)\,d\theta + \frac{1}{k(t)}\int_{t_0}^{t} k(\theta)\,dW(\theta)\right\}.$$

Note that Eq. (A.3) defines a Markovian process, so its finite-dimensional distributions depend on the initial distribution and on the transition probability density function (pdf). Moreover, following [1], $Z(t)$ is a Gaussian process if and only if the initial state Z_0 is a normal (or

degenerate) random variable. In such cases the mean and covariance functions of $Z(t)$ are given by

$$m_Z(t) = \mathbb{E}(Z_0) + \frac{1}{\sigma}\int_{t_0}^{t} k(\theta)\left[\alpha - C(\theta) - \frac{\sigma^2}{2}\right] d\theta,$$
$$R_Z(s,t) = Var(Z_0) + \int_{t_0}^{s\wedge t} k^2(\theta)\, d\theta, \quad \text{with } s\wedge t = \min(s,t),$$

respectively. In particular, the variance function of $Z(t)$ is

$$\sigma_Z^2(t) = Var(Z_0) + \int_{t_0}^{t} k^2(\theta)\, d\theta.$$

The finite dimensional distributions of $Z(t)$ are normal, that is, for $n \in N$

$$(Z(t_1), Z(t_2), \ldots, Z(t_n))' \sim \mathcal{N}_n(\mu, \Sigma),$$

where the i-th component of the vector μ is $m_Z(t_i)$, $i = 1, 2, \ldots, n$, and Σ is a definite positive matrix with components $R_Z(t_i, t_j)$, $i, j = 1, 2, \ldots, n$.
Therefore, from (A.1) we can conclude that the finite dimensional distributions of $X(t)$ are lognormal:

$$(X(t_1), X(t_2), \ldots, X(t_n))' \sim \Lambda_n(\eta, \Delta), \tag{A.4}$$

where the components of the vector η and of the matrix Δ are given by

$$\eta_i = \frac{\sigma}{k(t_i)}\, m_Z(t_i), \qquad \delta_{ij} = \frac{\sigma^2}{k(t_i)\, k(t_j)}\, R_Z(t_i, t_j),$$

respectively. From (A.4), the conditioned distributions can be obtained. In particular, the transition pdf is given by (2.7).